

Received July 11, 2019, accepted August 8, 2019, date of publication August 21, 2019, date of current version August 30, 2019.

Digital Object Identifier 10.1109/ACCESS.2019.2936036

# Physical Layer Security Performance Analysis of the FD-Based NOMA-VC System

WENWU XIE<sup>1</sup>, JIANWU LIAO<sup>1</sup>, CHAO YU<sup>1,2</sup>, PENG ZHU<sup>1</sup>, AND XINZHONG LIU<sup>1</sup>

<sup>1</sup>School of Information Science and Engineering, Hunan Institute of Science and Technology, Yueyang 414006, China

<sup>2</sup>Department of Information and Communication Engineering, Hoseo University, Asan 31066, South Korea

Corresponding author: Xinzhong Liu (80841895@qq.com)

This work was supported in part by the Science and Technology Program of Hunan Province under Grant 2016TP1021, in part by the Natural Science Foundation of Hunan Province under Grant 2018JJ2154, Grant 2018JJ2151, Grant 2018JJ3210, and Grant 2018JJ2156, in part by the Outstanding Youth Project of Hunan Provincial Education Department under Grant 18B353, in part by the 13th Five-years Plan of Education Science Program of Hunan Province under Grant XJK17BXX004, in part by the Key Research Foundation of Education Bureau of Hunan Province under Grant 18A320, and in part by the Natural Science Foundation of China under Grant 61772195.

**ABSTRACT** In this paper, we consider the secrecy outage probability (SOP) of a cooperative non-orthogonal multiple access (NOMA) vehicular communication (VC) system, where the relay is working in either half-duplex (HD) or full-duplex (FD) mode. We assume that all these links experience Nakagami-m fading. Some closed-form analytical expressions for the SOP performance of the FD/HD cooperative NOMA-VC system are derived. Results show that the secrecy performance of FD-based NOMA-VC system is superior than HD-based NOMA-VC in the low signal noise ratio (SNR) region, and can be further improved by reducing the self-interference caused by FD technique. Finally, the validity of this analytical expressions is verified by using simulation. The simulation results show that the simulation curve can be fit well with our analytical results.

**INDEX TERMS** Physical layer security, non-orthogonal multiple access, cooperative communications, full/half duplex relaying, vehicular communication.

## I. INTRODUCTION

The goal of the fifth generation (5G) networks is that the data rate should achieve a ten-fold increase in the connection density [1]. The non-orthogonal multiple access (NOMA) has been regarded as one of the promising key technology to enhance the spectral efficiency (SE) and improve the data rate of the 5G wireless networks [2]. Unlike the conventional orthogonal multiple access (OMA) structures, such as frequency division multiple access (FDMA), time division multiple access (TDMA), etc., the core idea of NOMA is to multiplex additional users in the same time / frequency / space resources but different power allocation [3]. Due to the above-mentioned advantages of the NOMA, the NOMA is suggested to be applied in the practical networks. The paper [4] explored NOMA in millimeter-wave communications and obtained the maximization of the sum data rate of a two-user millimeter-wave-NOMA system. The paper [5] investigated the power control and channel assignment problem in device-to-device (D2D) NOMA communication system equipped

with NOMA, which aim to maximize the sum data rate of D2D pairs and guarantee the minimum rate to achieve the requirements of NOMA-based users.

Recently, considering the advantages of NOMA, it becomes a focus of research on applying NOMA in VC networks, which can support the high quality-of-service (QoS) requirements of vehicular communication (VC). The literature [6] discussed the challenges and potentials for NOMA in 5G-enabled vehicular networks. Chen *et al.* [7] proposed an effective interference hypergraph-based resource allocation (IHG-RA) scheme for NOMA-VC system with complicated interference.

The VC enables the information transmission between vehicles or with other objects. The VC plays a key role in improving the road effectiveness and safety, which lays the foundation for future smart transport systems and is developed as an indispensable part of the intelligent transportation system (ITS) [7]. Furthermore, lacking of secure vehicles system might result in attacks or accident, which serious damage ITS efficiency and threaten driving safety [8]. This promotes the secure aspects of VC research.

The associate editor coordinating the review of this article and approving it for publication was Zheli Liu.

Given the broadcast nature of wireless transmissions, the concept of physical layer security (PLS) was initially discussed by Wyner in [10]. The PLS schemes exploit the randomness of wireless fading channel rather than cryptography techniques to improve the security of communication system [11]. Considering PLS in NOMA system has also attracted numerous researcher interests. The work in [12] first studied the secure transmission in NOMA system. Optimal power allocation scheme to maximize the secrecy sum rate is proposed. In [13], the exact and asymptotic expressions for secrecy outage probability of NOMA network under multiple-antenna and single-antennas scenarios were derived. In [14], PLS was studied in multi-antenna NOMA scenario with different transmit antenna selection (TAS) strategies. Later, [15] analyzed the secrecy outage probability (SOP) for MIMO-NOMA experience Nakagami-m fading channel with max-min TAS scheme. The secrecy analysis of a cooperative NOMA system was investigated in [16], where both amplify-and-forward (AF) and decode-and-forward (DF) relaying strategy were considered. The authors of [17] employed the FD and artificial noise (AN) techniques in a secure NOMA-based two-way relay network. The closed-form expressions for the ergodic secrecy rate were derived under both exclud-ing and involving eavesdroppers. To the best of the authors' knowledge, the secrecy performance of the NOMA-based VC has not been studied from the physical layer perspective.

In this paper, we study the SOP of the NOMA-based VC under the Nakagami-m fading channel and adopt FD technique at the relay. In addition, we derived some new closed-form analytical expressions for the SOP of the proposed FD-based NOMA-based VC system. The simulation results show that, with good self-interference cancellation, the SOP of FD NOMA-based VC system is better than that of HD NOMA-based VC system.

## II. SYSTEM AND CHANNEL MODEL

In this paper, we consider a downlink cooperative NOMA-based VC system including one base station (BS), one DF relay (Relay-1), a pair of users (i.e. D1, Vehicle-A, strong user, and D2, Vehicle-B, weak user) and an eavesdropper (Eve), as shown in Fig. 1. The relay is equipped with two antennas to enable FD to operate, while the BS, users and Eve only equip with one single antenna. Another, assuming that there is no direct link between the BS and users, as well as Eve and all the BS-relay, relay-user and relay-E channels experience independent and identically distributed Nakagami-m fading. As FD technique is employed, the relay undergoes severe self-interference (SI). Similar to [16], we assume that the SI cannot be suppressed completely under FD operation, and an actual value should be set. Furthermore, the SI channel is assumed to be free of fading.

During the  $l$ -th time slot, where  $l = 1, 2, 3 \dots$ , the BS will transmit the superimposed signal  $\sqrt{a_1}x_1[l] + \sqrt{a_2}x_2[l]$ , where  $x_i(i = 1, 2)$  denotes the united power signal for  $D_i$  and  $a_i$  denotes the power allocation coefficient. To fulfill  $D_1$ 's quality of service, we assume that  $a_2 \geq a_1$  with  $a_2 + a_1 = 1$ .

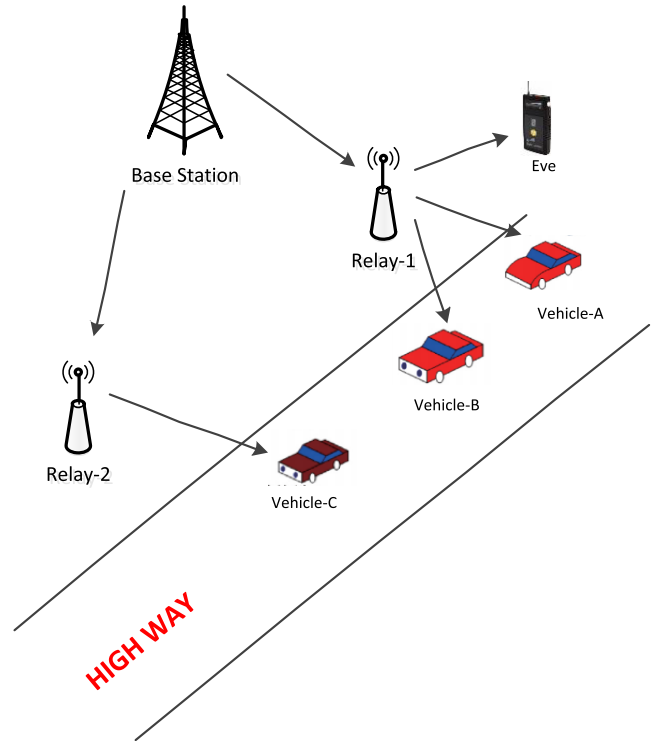


FIGURE 1. System model.

Then, the received signal at the relay is given by

$$y_R = h_{SR} (\sqrt{a_1}x_1[l] + \sqrt{a_2}x_2[l]) + \varpi s_r + n_r \quad (1)$$

where  $h_{SR}$  denotes the channel coefficient between the BS and relay,  $n_r$  denotes additive white Gaussian noise (AWGN) and  $s_r$  denotes the residual SI due to FD mode.  $\varpi$  is the switching operation factor, where  $\varpi = 1$  denotes the relay working in FD mode, while  $\varpi = 0$  denotes the HD mode.

For the DF relaying, the relay first decodes its received superimposed signal from BS through NOMA protocol and then re-encodes and forwards it to the destination. Based on the mentioned above information, the received signal-to-interference-plus-noise ratio (SINR) at the relay to decode  $x_1$  and  $x_2$  can be obtained as following

$$\gamma_{D_2 \rightarrow R} = \frac{\rho_{D_2} a_2 |h_{SR}|^2}{\rho_{D_1} a_1 |h_{SR}|^2 + \varpi \gamma_{SI} + 1} \quad (2)$$

and

$$\gamma_{D_1 \rightarrow R} = \frac{\rho_{D_1} a_1 |h_{SR}|^2}{\varpi \gamma_{SI} + 1} \quad (3)$$

where  $\rho$  is the transmit SNR, and  $\gamma_{SI} = |s_r|^2$ , for the SI channel is free of fading.

Assuming that the relay can decode the two signals successfully. Then, the observation at  $D_i$  and E can be expressed as

$$y_\theta = h_\theta (\sqrt{a_1}x_1[l-1] + \sqrt{a_2}x_2[l-1]) + n_\theta \quad (4)$$

where  $\theta \in \{D_1, D_2, E\}$ ,  $h_\theta$  denotes the channel coefficient between relay and  $\theta$ , and  $n_\theta$  denotes the AWGN.

After receiving the signal,  $D_2$  decodes its own message  $x_2$ , by treating  $x_1$  as noise. Then, the received SINR at  $D_2$

to decode its own signal is given by

$$\gamma_{D_2} = \frac{\rho_D a_2 |h_{D_2}|^2}{\rho_D a_1 |h_{D_2}|^2 + 1} \quad (5)$$

Simultaneously, D1 first decodes  $x_2$  and then obtain its own message using NOMA protocol. As such, the received SINR at D1 to decode  $x_2$  and  $x_1$  are given by

$$\gamma_{D_2 \rightarrow D_1} = \frac{\rho_D a_2 |h_{D_1}|^2}{\rho_D a_1 |h_{D_1}|^2 + 1} \quad (6)$$

and

$$\gamma_{D_1} = \rho_D a_1 |h_{D_1}|^2 \quad (7)$$

respectively.

In this paper, we consider the worst-case scenario, in which the multiuser data stream is received from the BS, which can be wiretapped by the Eve [9]. Therefore, the SNR for Eve to detect the information of  $D_i$ , where  $i = 1, 2$  can be expressed as

$$\gamma_{E_i} = \rho_E a_i |h_E|^2 \quad (8)$$

where  $h_E$  denotes the channel coefficient between relay and Eve and  $\rho_E$  is the transmit SNR at Eve. To simplify analysis, we assume  $\rho_D = \rho_E = \rho$ .

Since all links undergo Nakagami-m fading, the cumulative distribution function (CDF) and probability density function (PDF) of channel gain  $x_i = |h_i|^2$  are given by

$$f_{x_i}(x) = \frac{(\beta_i)^{m_i} x^{m_i-1}}{\Gamma(m_i)} e^{-\beta_i x} \quad (9)$$

$$F_{x_i}(x) = 1 - \sum_{i=0}^{m_i-1} \frac{(\beta_i x)^i}{i!} e^{-\beta_i x} \quad (10)$$

where  $\Gamma(s) = \Gamma(s, 0)$  is the Gamma function [19],  $\beta_i = m_i/\Omega_i$ ,  $m_i$  denotes the fading factor, and  $\Omega_i = E\{x_i\}$ .

### III. SIMULATION RESULTS

In this part, we evaluate the SOP performance of the cooperative NOMA-VC system under perfect channel state information (CSI). The SOP performance is the likelihood of achieving a non-negative target secrecy rate and can be formulated as [6]

$$P_{out} = Pr(\lceil C_D - C_E \rceil^+ < R_s) \quad (11)$$

where  $\lceil x \rceil^+ = \max\{x, 0\}$ ,  $R_s$  is the target secrecy rate,  $C_D$  and  $C_E$  are the channel capacities of the main and the wiretap link, respectively. With the above definition, the SOP of the FD-based cooperative NOMA-VC system can be expressed as:

$$\begin{aligned} SOP &= Pr(\lceil C_{D_1} - C_{E_1} \rceil^+ < R_{s_1} \text{ or } \lceil C_{D_2} - C_{E_2} \rceil^+ < R_{s_2}) \\ &= 1 - Pr\left(\left[\frac{1 + \bar{\gamma}_1}{1 + \gamma_{E_1}}\right]^{++} > \varepsilon_1, \left[\frac{1 + \bar{\gamma}_2}{1 + \gamma_{E_2}}\right]^{++} > \varepsilon_2\right) \end{aligned} \quad (12)$$

where  $\bar{\gamma}_1 = \min\{\gamma_{D_1 \rightarrow R}, \gamma_{D_1}\}$ ,  $\bar{\gamma}_2 = \min\{\gamma_{D_2 \rightarrow R}, \gamma_{D_2}, \gamma_{D_2 \rightarrow D_1}\}$ , and  $\varepsilon_i = 2^{R_{s_i}}$ . It is noted that the variables  $\bar{\gamma}_1, \bar{\gamma}_2,$

$\gamma_{E_1}$  and  $\gamma_{E_2}$  in (12) are correlated, which makes it difficult to obtain an exact expression for the SOP. Hence, by employing basic probability theory, an upper bound of SOP is given as

$$\begin{aligned} SOP &\leq \min\left\{1, 2 - pr\left(\frac{1 + \bar{\gamma}_1}{1 + \gamma_{E_1}} > \varepsilon_1\right) - pr\left(\frac{1 + \bar{\gamma}_2}{1 + \gamma_{E_2}} > \varepsilon_2\right)\right\} \\ &= \min\left\{1, \underbrace{pr\left(\frac{1 + \bar{\gamma}_1}{1 + \gamma_{E_1}} < \varepsilon_1\right)}_{p_1^{out}} + \underbrace{pr\left(\frac{1 + \bar{\gamma}_2}{1 + \gamma_{E_2}} < \varepsilon_2\right)}_{p_2^{out}}\right\} \end{aligned} \quad (13)$$

The term  $p_i^{out}$  in (13) represented the SOP at  $D_i$  and can be calculated as follow:

$$\begin{aligned} p_i^{out} &= pr(\bar{\gamma}_i < \varepsilon_i(1 + \gamma_{E_i}) - 1) \\ &= \int_0^\infty f_{\gamma_{E_i}}(x) F_{\bar{\gamma}_i}(\varepsilon_i(1 + x) - 1) dx \end{aligned} \quad (14)$$

In order to obtain the SOP at each user, we first derive the channel statistics for users and Eve. According to (3), (7) and (10), the CDF of  $\bar{\gamma}_1$  can be derived as follow:

$$\begin{aligned} F_{\bar{\gamma}_1}(x) &= pr(\min\{\gamma_{D_1 \rightarrow R}, \gamma_{D_1}\} < x) \\ &= 1 - pr(\gamma_{D_1 \rightarrow R} > x) pr(\gamma_{D_1} > x) \\ &= 1 - \left(1 - F_{|h_{SR}|^2}\left(\frac{\rho \varpi \gamma_{SI} + 1}{\rho a_1} x\right)\right) \\ &\quad \times \left(1 - F_{|h_{D_1}|^2}\left(\frac{x}{\rho a_1}\right)\right) \\ &= 1 - \sum_{i=0}^{m_R-1} \sum_{j=0}^{m_D-1} A_{ij} x^{i+j} e^{-\frac{C_1 x}{\rho a_1}} \end{aligned} \quad (15)$$

where

$$\begin{aligned} A_{ij} &= \frac{(1 + \rho \varpi \gamma_{SI})^i \beta_R^i \beta_{D_1}^j}{i! \cdot j! \cdot (\rho a_1)^{i+j}} \\ C_1 &= \beta_R(1 + \rho \varpi \gamma_{SI}) + \beta_{D_1} \end{aligned}$$

In similar, the CDF of  $\bar{\gamma}_2$  and PDF of  $\gamma_{E_i}$  are given as:

$$F_{\bar{\gamma}_2}(x) = \begin{cases} 1 - \sum_{i=0}^{m_R-1} \sum_{j=1}^{m_{D_1}-1} \sum_{k=1}^{m_{D_2}-1} \frac{x^{i+j+k}}{i+j+k} \times B_{ijk} \left(\frac{\rho(a_2 - a_1 x)}{\rho a_1}\right) \\ \times e^{\frac{C_2 x}{\rho(a_2 - a_1 x)}}, & x \leq \frac{a_2}{a_1} \\ 1, & x > \frac{a_2}{a_1} \end{cases} \quad (16)$$

$$f_{E_i}(x) = \frac{\beta_E^{m_E} \left(\frac{x}{\rho a_i}\right)^{m_E-1}}{\Gamma(m_E)} e^{-\frac{\beta_E x}{\rho a_i}} \quad (17)$$

respectively, where

$$B_{ijk} = \frac{(1 + \rho\varpi \gamma_{SI})^i \beta_R^i \beta_{D_1}^j \beta_{D_2}^k}{i! \cdot j! \cdot k!}$$

$$C_2 = C_1 + \beta_{D_2}$$

Then, substituting (15) and (17) into (14) and making use of [20, eq. (3.351.3)],  $p_1^{out}$  can be derived as follow

$$p_1^{out} = \int_0^\infty \frac{\beta_E^{m_E} x^{m_E-1}}{\Gamma(m_E)(\rho_E a_1)^{m_E}} e^{-\frac{\beta_E x}{\rho_E a_1}}$$

$$\times (1 - \sum_{i=0}^{m_R-1} \sum_{j=0}^{m_{D_1}-1} A_{ij}(\varepsilon_1(1+x) - 1)^{i+j}$$

$$\times e^{-\frac{C_1(\varepsilon_1(1+x) - 1)}{\rho a_1}}) dx$$

$$= 1 - \frac{\beta_E^{m_E} e^{-\frac{C_1(\varepsilon_1-1)}{\rho_E a_1}}}{\Gamma(m_E)(\rho_E a_1)^{m_E}} \sum_{i=0}^{m_R-1} \sum_{j=0}^{m_{D_1}-1} A_{ij}$$

$$\times \sum_{j=1}^{m_{D_1}-1} \binom{i+j}{k} \times (k + m_E - 1)!$$

$$\times \varepsilon_1^k (\varepsilon_1 - 1)^{i+j-k} \times \left(\frac{C_1 \rho_E \varepsilon_1 - \rho \beta_E}{\rho \rho_E a_1}\right)^{-k-m_E} \quad (18)$$

Making use of (14), the SOP at D<sub>2</sub> can be rewritten as

$$p_2^{out} = \int_0^\mu f \gamma_{E_2}(x) F_{\bar{\gamma}_2}(\varepsilon_2(1+x) - 1) dx + \int_\mu^\infty f \gamma_{E_2}(x) dx \quad (19)$$

where  $\mu = \frac{1}{a_1 \eta_2} - 1$ .

Substituting (16) and (17) into (19), by employing Gaussian-Chebyshev quadrature, the SOP at D<sub>2</sub> is derived as

$$p_2^{out} = 1 - \int_0^\mu \frac{\beta_E^{m_E} x^{m_E-1}}{\Gamma(m_E)(\rho_E a_2)^{m_E}} e^{-\frac{\beta_E x}{\rho_E a_2}}$$

$$\times \sum_{i=0}^{m_E-1} \sum_{j=0}^{m_{D_1}-1} \sum_{k=0}^{m_{D_1}-1} B_{ijk}$$

$$\times \left(\frac{(\varepsilon_2 x + \varepsilon_2 - 1)}{(\rho(a_2 - a_1(\varepsilon_2 x + \varepsilon_2 - 1)))}\right)^{i+j+k}$$

$$\times e^{-\frac{C_2(\varepsilon_2 x + \varepsilon_2 - 1)}{\rho(a_2 - a_1(\varepsilon_2 x + \varepsilon_2 - 1))}} dx$$

$$\approx 1 - \frac{\beta_E^{m_E} x^{m_E-1}}{\Gamma(m_E)(\rho_E a_2)^{m_E}} e^{-\frac{\beta_E x}{\rho_E a_2}} \sum_{i=0}^{m_E-1} \sum_{j=0}^{m_{D_1}-1}$$

$$\times \sum_{k=0}^{m_{D_1}-1} B_{ijk} \times \frac{\mu \pi}{2N} \sum_{p=0}^N \sqrt{1 - \phi_p^2} \varphi\left(\frac{\mu \phi + \mu}{2}\right) \quad (20)$$

where  $\phi_p = \cos\left(\frac{2p-1}{2n}\pi\right)$ , and

$$\varphi(x) = x^{m_E-1} \left(\frac{(\varepsilon_2 x + \varepsilon_2 - 1)}{(\rho(a_2 - a_1(\varepsilon_2 x + \varepsilon_2 - 1)))}\right)^{i+j+k}$$

$$\times e^{-\frac{\beta_E x}{\rho_E a_2} - \frac{C_2(\varepsilon_2 x + \varepsilon_2 - 1)}{\rho(a_2 - a_1(\varepsilon_2 x + \varepsilon_2 - 1))}}$$

Finally, by substituting (18) and (20) into (13), the upper bound of SOP for the cooperative NOMA system under FD model is approximated by (21), as shown at the top of the next page.

For the special case  $\varpi = 0$ , the approximated expression of SOP for the HD-based NOMA system is given by (22), as shown at the top of the next page, where  $\eta_i = 2^{2R_{si}}$ ,

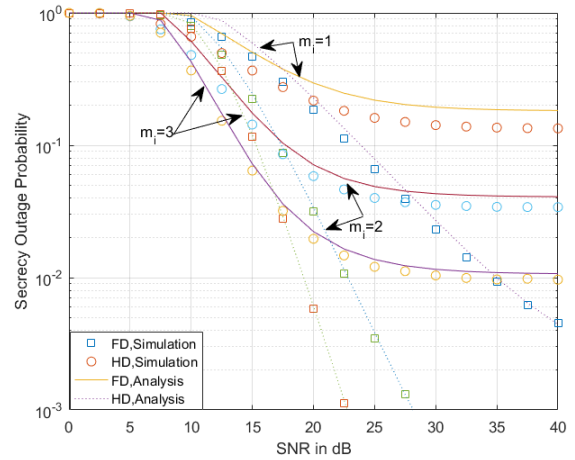


FIGURE 2. Secrecy outage probability versus SNR for different fading severity parameters with  $\rho_E = 0$  dB  $a_1 = 0.14$ ,  $R_{s1} = 0.5$ ,  $R_{s2} = 0.1$ BPCU and  $\gamma_{SI} = -15$ dB.

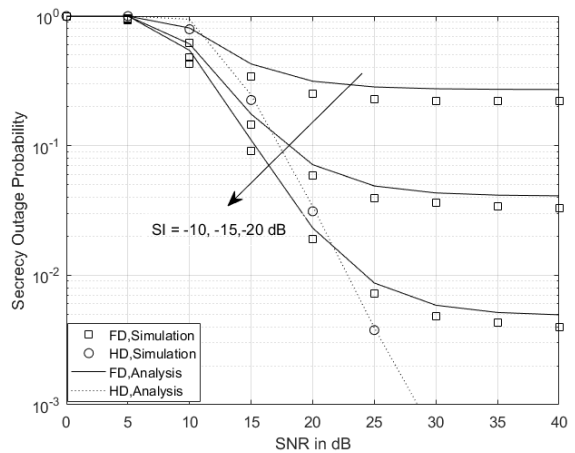


FIGURE 3. Secrecy outage probability versus SNR for different values of SI with  $\rho_E = 0$  dB  $a_1 = 0.14$ ,  $R_{s1} = 0.5$ ,  $R_{s2} = 0.1$ BPCU and  $m_i = 2$ .

$$A'_{ij} = \frac{\beta_R^i \beta_{D_1}^j}{i! \cdot j! \cdot (\rho a_1)^{i+j}}, B'_{ijk} = \frac{\beta_R^i \beta_{D_1}^j \beta_{D_2}^k}{i! \cdot j! \cdot k!}, C'_1 = \beta_R + \beta_{D_1}, C'_2 = C'_1 + \beta_{D_2}$$

$$\text{and } \varphi'(x) = x^{m_E-1} \left(\frac{(\eta_2 x + \eta_2 - 1)}{(\rho(a_2 - a_1(\eta_2 x + \eta_2 - 1)))}\right)^{i+j+k}$$

$$\times e^{-\frac{\beta_E x}{\rho_E a_2} - \frac{C'_2(\eta_2 x + \eta_2 - 1)}{\rho(a_2 - a_1(\eta_2 x + \eta_2 - 1))}}$$

#### IV. SIMULATION RESULTS

In this section, we will present some simulation results for the SOP of the cooperative NOMA-VC system under both FD and HD model. We assume  $\gamma_{SI} = -15$ dB and  $i \in \{r, D_1, D_2, E\}$ . The complexity-vs-accuracy tradeoff parameter is  $N = 50$ .

Fig. 2 plots the SOP of cooperative NOMA-VC system versus SNR for a simulation setting with  $\gamma_{SI} = -15$ dB. The case of fading severity parameter  $m_i = 1$  (Rayleigh fading),  $m_i = 2$  and  $m_i = 3$  for  $i \in \{r, D_1, D_2, E\}$ , which are considered. We can observe that the FD-based NOMA achieves a superior secrecy outage performance in the low SNR region. The reason is that the HD-based NOMA-VC system needs more communication resources to maintain the same secrecy performance. It is worth noting that the SOP of

$$\begin{aligned}
 SOP_{FD}^{ub} &= 1 - \frac{\beta_E^{m_E} e^{-\frac{c_1(\varepsilon_1-1)}{\rho_E a_1}}}{\Gamma(m_E)(\rho_E a_1)^{m_E}} \sum_{i=0}^{m_R-1} \sum_{j=0}^{m_{D_1}-1} A_{ij} \sum_{k=0}^{i+j} \binom{i+j}{k} (k+m_E-1)! \cdot \varepsilon_1^k (\varepsilon_1-1)^{i+j-k} \\
 &\times \left(\frac{\rho_E c_1 \varepsilon_1 - \rho \beta_E}{\rho \rho_E a_1}\right)^{-k-m_E} \frac{\beta_E^{m_E} x^{m_E-1}}{\Gamma(m_E)(\rho_E a_2)^{m_E}} \sum_{i=0}^{m_E-1} \sum_{j=0}^{m_{D_1}-1} \sum_{k=0}^{m_{D_2}-1} \\
 &\times B_{ijk} \frac{\mu \pi}{2N} \sum_{P=0}^N \sqrt{1 - \phi_P^2} \varphi\left(\frac{\mu \phi_P + \mu}{2}\right)
 \end{aligned} \tag{21}$$

$$\begin{aligned}
 SOP_{HD}^{ub} &= 1 - \frac{\beta_E^{m_E} e^{-\frac{c'_1(\eta_1-1)}{\rho_E a_1}}}{\Gamma(m_E)(\rho_E a_1)^{m_E}} \sum_{i=0}^{m_R-1} \sum_{j=0}^{m_{D_1}-1} A'_{ij} \sum_{k=0}^{i+j} \binom{i+j}{k} (k+m_E-1)! \cdot \eta_1^k (\eta_1-1)^{i+j-k} \\
 &\times \left(\frac{\rho_E c'_1 \eta_1 - \rho \beta_E}{\rho \rho_E a_1}\right)^{-k-m_E} \frac{\beta_E^{m_E} x^{m_E-1}}{\Gamma(m_E)(\rho_E a_2)^{m_E}} \sum_{i=0}^{m_E-1} \sum_{j=0}^{m_{D_1}-1} \sum_{k=0}^{m_{D_2}-1} \\
 &\times B'_{ijk} \frac{\mu \pi}{2N} \sum_{P=0}^N \sqrt{1 - \phi_P^2} \varphi'\left(\frac{\mu \phi_P + \mu}{2}\right)
 \end{aligned}$$

$$\begin{aligned}
 SOP &= pr \left( \left[ C_{D_1} - C_{E_1} \right]^+ < R_{s_1} \text{ or } \left[ C_{D_2} - C_{E_2} \right]^+ < R_{s_2} \right) \\
 &= 1 - pr \left( \left[ C_{D_1} - C_{E_1} \right]^+ > R_{s_1} \text{ and } \left[ C_{D_2} - C_{E_2} \right]^+ > R_{s_2} \right) \\
 &= 1 - pr \left( \left[ \min \{ \log_2(1 + \gamma_{D_1 \rightarrow R}), \log_2(1 + \gamma_{D_1}) \} - \log_2(1 + \gamma_{E_1}) \right]^+ > R_{s_1} \text{ and } \right. \\
 &\quad \left. \left[ \min \{ \log_2(1 + \gamma_{D_2 \rightarrow R}), \log_2(1 + \gamma_{D_2}) \} - \log_2(1 + \gamma_{E_2}) \right]^+ > R_{s_2} \right) \\
 &= 1 - pr \left( \left[ \frac{1 + \min \{ \gamma_{D_1 \rightarrow R}, \gamma_{D_1} \}}{1 + \gamma_{E_1}} \right]^{++} > 2^{R_{s_1}} \text{ and } \left[ \frac{1 + \min \{ \gamma_{D_2 \rightarrow R}, \gamma_{D_2} \}}{1 + \gamma_{E_2}} \right]^{++} > 2^{R_{s_2}} \right) \\
 &= 1 - pr \left( \left[ \frac{1 + \bar{\gamma}_1}{1 + \gamma_{E_1}} \right]^{++} > \varepsilon_1, \left[ \frac{1 + \bar{\gamma}_2}{1 + \gamma_{E_2}} \right]^{++} > \varepsilon_2 \right)
 \end{aligned} \tag{22}$$

the FD cooperative NOMA-VC system quickly saturates in the high SNR region. The main reason is that there is the SI in FD NOMA-VC system.

Fig. 3 plots the SOP of cooperative NOMA-VC system versus SNR with  $\gamma_{SI} = -20, -15, -10dB$ . We can observe that the secrecy performance of FD-based NOMA-VC is greatly affected by the value of SI, while little impact on HD-based NOMA-VC system, which is due to the fact that SI does not exist in HD-based NOMA-VC system. As the SI increases, the secrecy outage performance of the FD NOMA become worse. As a result, it is important for us consider the impact of SI when designing practical FD cooperative NOMA-VC system.

**V. CONCLUSION**

This paper investigated the SOP of a NOMA-based VC system, where all the channels undergo Nakagami-m fading. Some analytical expressions for SOP of both FD-based and HD-based NOMA have been derived. Simulation results show that the FD NOMA-based VC system outperforms the HD NOMA-based VC system on the condition of low SNR region, and also verify the analytical expressions correct. Results also reveal that the performance gain between FD and HD could be further improved by reducing the self-interference at the relay. The major weakness of this proposed method is that the velocity of the car is not considered, which is our next research point.

**APPENDIX**

Equation (12) derivation process, as *SOP*, as shown at the top of this page.

Equation (13) derivation process

$$\begin{aligned}
 SOP &= 1 - pr \left( \left[ \frac{1 + \bar{\gamma}_1}{1 + \gamma_{E_1}} \right]^{++} > \varepsilon_1, \left[ \frac{1 + \bar{\gamma}_2}{1 + \gamma_{E_2}} \right]^{++} > \varepsilon_2 \right) \\
 &\leq 2 - pr \left( \left[ \frac{1 + \bar{\gamma}_1}{1 + \gamma_{E_1}} \right]^{++} > \varepsilon_1 \right) \\
 &\quad - pr \left( \left[ \frac{1 + \bar{\gamma}_2}{1 + \gamma_{E_2}} \right]^{++} > \varepsilon_2 \right) \\
 &= \min \left\{ 1, 2 - pr \left( \frac{1 + \bar{\gamma}_1}{1 + \gamma_{E_1}} > \varepsilon_1 \right) \right. \\
 &\quad \left. - pr \left( \frac{1 + \bar{\gamma}_2}{1 + \gamma_{E_2}} > \varepsilon_2 \right) \right\} \\
 &= \min \left\{ 1, pr \left( \frac{1 + \bar{\gamma}_1}{1 + \gamma_{E_1}} > \varepsilon_1 \right) + pr \left( \frac{1 + \bar{\gamma}_2}{1 + \gamma_{E_2}} > \varepsilon_2 \right) \right\}
 \end{aligned}$$

Equation (14) derivation process

$$\begin{aligned}
 p_i^{out} &= pr(\bar{\gamma}_i < \varepsilon_i(1 + \gamma_{E_i}) - 1) \\
 &= \int_0^\infty \int_0^{\varepsilon_i(1+x)-1} f_{\gamma_{E_i}}(x) \cdot f_{\bar{\gamma}_i}(y) dx dy \\
 &= \int_0^\infty f_{\gamma_{E_i}}(x) \int_0^{\varepsilon_i(1+x)-1} f_{\bar{\gamma}_i}(y) dy dx \\
 &= \int_0^\infty f_{\gamma_{E_i}}(x) F_{\bar{\gamma}_i}(\varepsilon_i(1+x) - 1) dx
 \end{aligned}$$

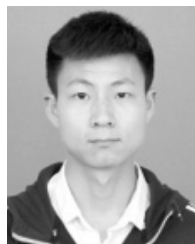


## REFERENCES

- [1] F. Boccardi, R. W. Heath, A. Lozano, T. L. Marzetta, and P. Popovski, "Five disruptive technology directions for 5G," *IEEE Commun. Mag.*, vol. 52, no. 2, pp. 74–80, Feb. 2014.
- [2] L. Dai, B. Wang, Y. Yuan, S. Han, C.-L. I, and Z. Wang, "Non-orthogonal multiple access for 5G: Solutions, challenges, opportunities, and future research trends," *IEEE Commun. Mag.*, vol. 53, no. 9, pp. 74–81, Sep. 2015.
- [3] Y. Sun, D. W. K. Ng, Z. Ding, and R. Schober, "Optimal joint power and subcarrier allocation for full-duplex multicarrier non-orthogonal multiple access systems," *IEEE Trans. Commun.*, vol. 65, no. 3, pp. 1077–1091, Mar. 2017.
- [4] Z. Xiao, L. Zhu, J. Choi, P. Xia, and X.-G. Xia, "Joint power allocation and beamforming for non-orthogonal multiple access (NOMA) in 5G millimeter wave communications," *IEEE Trans. Wireless Commun.*, vol. 17, no. 5, pp. 2961–2974, May 2018.
- [5] Y. Pan, C. Pan, Z. Yang, and M. Chen, "Resource allocation for D2D communications underlying a NOMA-based cellular network," *IEEE Wireless Commun. Lett.*, vol. 7, no. 1, pp. 130–133, Feb. 2018.
- [6] B. Di, L. Song, Y. Li, and Z. Han, "V2X meets NOMA: Non-orthogonal multiple access for 5G-enabled vehicular networks," *IEEE Wireless Commun.*, vol. 24, no. 6, pp. 14–21, Dec. 2017.
- [7] C. Chen, B. Wang, and R. Zhang, "Interference hypergraph-based resource allocation (IHG-RA) for NOMA-integrated V2X networks," *IEEE Internet Things J.*, vol. 6, no. 1, pp. 161–170, Feb. 2019.
- [8] L. Li, D. Wen, and D. Yao, "A survey of traffic control with vehicular communications," *IEEE Trans. Intell. Transp. Syst.*, vol. 15, no. 1, pp. 425–432, Feb. 2014.
- [9] M. Azees, P. Vijayakumar, and L. J. Deborah, "Comprehensive survey on security services in vehicular ad-hoc networks," *IET Intell. Transp. Syst.*, vol. 10, no. 6, pp. 379–388, Aug. 2016.
- [10] A. D. Wyner, "The wire-tap channel," *Bell Syst. Tech. J.*, vol. 54, no. 8, pp. 1355–1387, Oct. 1975.
- [11] F. Jameel, S. Wyne, G. Kaddoum, and T. Q. Duong, "A comprehensive survey on cooperative relaying and jamming strategies for physical layer security," *IEEE Commun. Surveys Tuts.*, to be published.
- [12] Y. Zhang, H.-M. Wang, Q. Yang, and Z. Ding, "Secrecy sum rate maximization in non-orthogonal multiple access," *IEEE Commun. Lett.*, vol. 20, no. 5, pp. 930–933, May 2016.
- [13] Y. Liu, Z. Qin, M. Elkashlan, Y. Gao, and F. L. Hanzo, "Enhancing the physical layer security of non-orthogonal multiple access in large-scale networks," *IEEE Trans. Wireless Commun.*, vol. 16, no. 3, pp. 1656–1672, Mar. 2017.
- [14] H. Lei, J. Zhang, K.-H. Park, P. Xu, I. S. Ansari, G. Pan, B. Alomair, and M.-S. Alouini, "On secure NOMA systems with transmit antenna selection schemes," *IEEE Access*, vol. 5, pp. 17450–17464, 2017.
- [15] H. Lei, J. Zhang, K.-H. Park, P. Xu, Z. Zhang, G. Pan, and M.-S. Alouini, "Secrecy outage of max–min TAS scheme in MIMO-NOMA systems," *IEEE Trans. Veh. Technol.*, vol. 67, no. 8, pp. 6981–6990, Aug. 2018.
- [16] J. Chen, L. Yang, and M.-S. Alouini, "Physical layer security for cooperative NOMA systems," *IEEE Trans. Veh. Technol.*, vol. 67, no. 5, pp. 4645–4649, May 2018.
- [17] B. Zheng, M. Wen, C.-X. Wang, X. Wang, F. Chen, J. Tang, and F. Ji, "Secure NOMA based two-way relay networks using artificial noise and full duplex," *IEEE J. Sel. Areas Commun.*, vol. 36, no. 7, pp. 1426–1439, Jul. 2018.
- [18] Y. Ai, A. Mathur, M. Cheffena, and M. R. Bhatnagar, "On physical layer security of double Rayleigh fading channels for vehicular communications," *IEEE Wireless Commun. Lett.*, vol. 7, no. 6, pp. 1038–1041, Jul. 2018.
- [19] N. Guo, J. Ge, C. Zhang, Q. Bu, and P. Tian, "Non-orthogonal multiple access in full-duplex relaying system with Nakagami- $m$  fading," *IET Commun.*, vol. 13, no. 3, pp. 271–280, Feb. 2019.
- [20] I. S. Gradshteyn and I. M. Ryzhik, *Table of Integrals, Series, and Products*, A. Jeffrey, Ed. San Diego, CA, USA: Academic, 2000.



**WENWU XIE** was born in Jingzhou, Hubei, China, in 1979. He received the B.S., M.S., and Ph.D. degrees in communication engineering from Huazhong Normal University, in 2004, 2007, and 2017, respectively. From 2007 to 2009, he was a Communication Algorithm Engineer with Spreadtrum Communication Company Ltd. Since 2012, he has been an Algorithm Manager with MediaTek Company Ltd. Since 2017, he has been a Lecturer with HNIST. He holds two patents. His research interests include communication algorithm, such as channel estimation, equalizer and encoding/decoding, and so on.



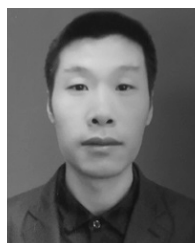
**JIANWU LIAO** was born in Hengyang, Hunan, China, in 1996. He received the B.S. degree from the School of Information Science and Engineering, HNIST, in 2018, where he is currently pursuing the master's degree. His major research interests include non-orthogonal multiple access and physical layer security.



**CHAO YU** was born in Yueyang, Hunan, China, in 1986. He received the B.S. degree in communication engineering from the Guilin University of Electronic Technology, in 2009 and 2012. He is currently pursuing the Ph.D. degree with Hoseo University, South Korea. Since 2012, he has been a Teacher with HNIST. His research interests include MIMO-NOMA physical layer security cooperative communications, mmWave communications, and so on.



**PENG ZHU** was born in Yueyang, Hunan, China, in 1990. He received the Ph.D. degree in space physics from Wuhan University. Since 2016, he has been a Lecturer with HNIST. His major research interests include signal processing and communication techniques.



**XINZHONG LIU** was born in 1978. He received the Ph.D. degree. His main research interests include software reliability analysis, computer communication security, and heterogeneous parallel computing.

...